

## Influence of ZrO<sub>2</sub> Particles on the Tribological Properties of AlMg5 Alloy

Rashed<sup>a\*</sup> G.M., Sadawy<sup>b</sup>, M.M., Kandil<sup>b</sup>, A., Abdelkareem<sup>a</sup>, A. and Mohrez<sup>a</sup>, W.A.

<sup>a</sup>- Reactor Materials Department, Nuclear Materials Authority, Cairo, Egypt

<sup>b</sup>-Mining and Petroleum Dept., Faculty of Engineering, Al-Azhar University, Nasr City, Cairo, Egypt

\*Corresponding author e-mail: [g.rashed010@gmail.com](mailto:g.rashed010@gmail.com)

### Abstract

Aluminum based metal matrix composites are devoting more interest towards multiple applications due to their good thermal and mechanical properties. At this study, composites of AlMg5/ZrO<sub>2</sub> with multiple gradients of ZrO<sub>2</sub>, were manufactured using stir casting technique. Microstructure, hardness and tribological properties of the composite were investigated. Pin-on-disk technique was used under wet conditions (3.5 wt. % NaCl solution) at different sliding speeds (varied from 0.125 to 0.5 ms<sup>-1</sup>) and applied loads (varied from 5 to 20N). Microstructure and X-Ray Diffraction (XRD) analysis show that the composites AlMg5/ZrO<sub>2</sub> were successfully manufactured via stir casting with a uniform distribution of ZrO<sub>2</sub> particles. The results revealed that the hardness and wear resistance of the investigated alloy significantly increased by incorporating ZrO<sub>2</sub> up to 10 wt.%, beyond this value the hardness and wear resistance diminished but still higher than the base alloy. Further, the outcomes showed that the dominant wear mechanism in AlMg5 alloy and its composite was the abrasive wear.

### Article Info

Received 18 Mar. 2021

Revised 16 May. 2021

Accepted 17 Jun. 2021

### Keywords

Al-MMCs; Zirconia; Stir Casting; Wet wear resistance.

### Introduction

Aluminum and its alloys are wide range applicable in aviation, automotive and defense sectors, due to their low density, durable mechanical properties and good corrosion resistance. However, relatively low wear resistance of aluminum and its alloys despite good mechanical properties restricts the use of these alloys in some tribological applications [1-3]. In order to overcome these drawbacks and to align with such elevated engineering demands of modern technology, the metal matrix composites (MMCs) are devoting more attention to be more applicable as an engineering material [4]. In recent years, aluminum metal matrix composites (Al-MMCs), have drawn more attention globally, due to their promising potential to replace their monolithic counterparts which are installed primarily in automobile and energy sector. Al-Mg alloys reinforced with ceramic particulates have significant potential for structural and marine applications due to their high stiffness and specific strength as well as low density [5]. There are several types of particles, whiskers or fibers ceramics that can be used as reinforcement media in composites such as SiC [6], Al<sub>2</sub>O<sub>3</sub> [7], TiC [8], WC [9] and diamond [10] according to the required application of the materials. Nowadays the particulate reinforced Al matrix composite are focused attentively by global industrial sector, because of their low cost with advantage of its isotropic-symmetric directions properties. In

comparison to other oxide ceramics, ZrO<sub>2</sub> has superior biomechanical properties (toughness, strength, and fatigue resistance, fracture strength, and low elasticity module), in addition to the excellent wear resistance and biocompatibility [11].

Different approaches of liquid-state, solid-state, and in-situ processing can be used in manufacturing of MMCs [12]. Stir casting or vortex casting is more suitable to produce near shaped final products. Hence, from the viewpoint of industrial applications and academic studies, vortex casting has drawn attentions to produce different MMCs with a unique structure and mechanical properties [13]. Khalili et al.[14] produced Al6061/ ZrO<sub>2</sub> with 3 and 6% of ZrO<sub>2</sub> by stirring casting process. Their outcomes showed the highest wear resistance was obtained with matrix has 3% ZrO<sub>2</sub>. Kumar et al. [15] manufactured A6061/ZrO<sub>2</sub> nano composite via stirring casting process. Wear test results showed that wear resistance of the MMCs improved as the content of nano-reinforcement increased. The production of Al- ZrO<sub>2</sub> composites by stirring casting is correlated with problems such as low wettability of ZrO<sub>2</sub> with molten Al, and a higher density of ZrO<sub>2</sub> compared to that of Al, which results in deposition and therefore a heterogeneous distribution of ZrO<sub>2</sub> particles [16]. Therefore, many authors preferred to use powder technique instead of stir casting to avoid these problems. For example, Şimşek et al. [2] fabricated Al 2% graphite/ZrO<sub>2</sub> composites with four different amounts of ZrO<sub>2</sub> up to 12% via powder metallurgy

technique then studied their wear behavior. The study showed that both hardness and density values increased as the amount of  $ZrO_2$  increased. In addition, Wear rate decreased with increasing amount of reinforcement in the matrix. However, liquid state processing such as stir casting has been considered as a flexible, simple and low cost one for manufacturing of MMCs compared to other routes. [17,18]. Therefore, the present study aims to manufacture Al-MMCs with incorporating different amounts of  $ZrO_2$  into AlMg5 alloy using stir casting technique. The study was also extended to investigate the effect of  $ZrO_2$  on the tribological properties of AlMg5/ $ZrO_2$  composites in wet conditions (3.5 wt. % NaCl solution).

## Materials and Methods

### Materials

In this present investigation, AlMg5 ingot and  $ZrO_2$  particles were used to prepare Al-MMCs. The composition of the as received base matrix (AlMg5) and  $ZrO_2$  are provided in Table 1. High purity Zirconia particles were obtained from the Egyptian Nuclear Materials Authority (ENMA) in micron scale where the average size of particles is 180  $\mu m$ .

**Table 1** Chemical composition (wt%) of materials.

Components (%)	Material	
	AlMg5	$ZrO_2$
Mg	4.89	----
Zr	----	91.8
Si	0.053	0.44
Mn	0.002	----
Fe	0.025	----
Cu	0.002	----
Hf	----	2.57
O	----	5.19
Al	Bal	----

### Fabrication method

Stir casting technique was used to manufacture the composites of AlMg5/ $ZrO_2$  with different amounts of  $ZrO_2$ , (5,10, and 15wt. %) as shown in Fig. 1. In respect to the stir casting challenges such as poor wettability and pushing of particles by molten metal,  $ZrO_2$  was chemically treated to enhance the wettability and to obtain uniform distribution of  $ZrO_2$  particles into the matrix. The manufacturing of Al-MMCs was started by melting in the electric furnace. About 300 g of the base matrix was first melted in a crucible and maintained till a homogeneous liquid phase is obtained at 100°C above its liquidous temperature. After melting, the molten melt was degassed by purging argon stream gas for 2 min., to get rid of the entrapped gases. This was followed by a skimming slag away from the melt surface. The mechanical stirrer was inserted below the surface to about 2/3 of the molten metal volume. The stirrer

rotates at an impeller speed 800 rpm to create the vortex which helps in the equilibrium mixing of matrix and reinforcement. At this stage, the activated  $ZrO_2$  particles were dispersed gradually at the rate approximately 30  $g \cdot min^{-1}$ . The melt was continuously stirred for 2 min and degassed after addition of the  $ZrO_2$  particles into melt to ensure gain a uniform distribution of particles through the matrix, the stirrer was then within drawn and the molten metal was poured at 700 °C into the metallic mold.

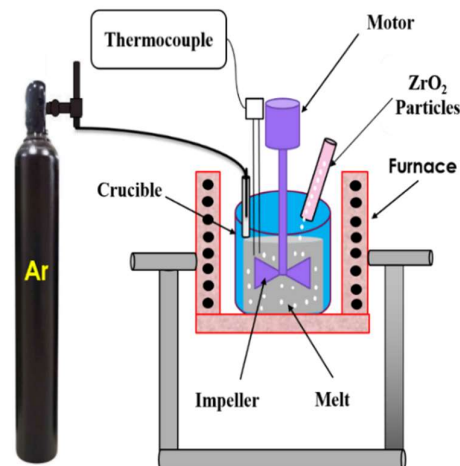


**Figure 1** A schematic diagram for stir casting aperture.

### Relative density

The relative densities ( $\rho_{rel}$ ) of AlMg5 and AlMg5/ $ZrO_2$  composites were determined according to Eq. (1):

$$\rho_{rel} = (\rho_{exp} / \rho_{th}) \times 100 \quad (1)$$

where  $\rho_{exp}$  and  $\rho_{th}$  are the experimental and theoretical densities ( $g/cm^3$ ) respectively. The experimental densities of AlMg5 and AlMg5/ $ZrO_2$  composite were determined using Archimedes' method [13]. The theoretical density ( $\rho_{th}$ ) of AlMg5 and AlMg5/ $ZrO_2$  composite were calculated according to Eq. (2) [14]:

$$\rho_{th} = (W_m \times \rho_m) + (W_r \times \rho_r) \quad (2)$$

where  $\rho_m$  and  $\rho_r$  are the densities of AlMg5 and  $ZrO_2$  in  $g/cm^3$ , while the  $W_m$  and  $W_r$  are their Weight percentage respectively.

### Microstructural evaluation

The microstructure of AlMg5 and AlMg5/ $ZrO_2$  composites and the distributions nature of  $ZrO_2$  in the matrix was evaluated by an optical microscope model (LECO-LX31-USA) with 500X maximum magnification, equipped with a (PAX-Cam) digital camera and (PAXIT) software. All ingots were firstly cut down into round shapes, and then were grinded on different grit size papers sequentially by 220, 500, 800 and 1200 respectively. After that, the specimens were mechanically polished by alumina paste (grade 1 and 0.3  $\mu m$ ). The surfaces of samples were cleaned using ethyl alcohol and dried in hot air.

## XRD

X-ray diffraction (XRD) analysis was conducted by using XRD device model (Malvern Panalytical Empyrean-2020 Netherlands) to determine the different phases of  $ZrO_2$  powders, AlMg5 base alloy, and AlMg5/ $ZrO_2$  composites. A monochromatic Cu-K radiation with  $\lambda = 0.154$  nm was used. The scanning range was 5–75 ( $2\theta$ ) with a step size of 0.02 ( $2\theta$ )/Sec.

## Hardness

In the present study Vickers microhardness test using a load of 300 gf for 10 seconds was conducted on AlMg5 and AlMg5/ $ZrO_2$  composites to determine their resistance for penetration of the indenter. Seven spot readings have been conducted on each sample by Vickers microhardness machine model (LECO LM70 - USA).

## Wet abrasive wear testing

The wet abrasive wear tests were conducted by using a pin-on-disc machine in 3.5 % wt. NaCl environment as shown in Fig. 2. The sliding speed was 0.125, 0.250, 0.375 and 0.5  $ms^{-1}$ , at constant load of 15 N, while the applied load was 5,10, 15, and 20 N at constant speed of 0.375  $ms^{-1}$ . The testing duration and size of abrasive material were 30 minutes and 13  $\mu m$ . The abrasive material (SiC paper) was fixed on an aluminum wheel covered with rubber. The load was applied on the specimen through a cantilever and the specimen was in contact with the rotating disc having a diameter of 140 mm.

Three separate experiments were conducted for each test to ensure the reproducibility. The standard deviation values were calculated to assess the statistical error for all tests. The specimens after each test were dried, cleaned with a soft brush and weighed with a micro-balance. The mass loss value of the samples was determined using an electronic balance of 0.1 mg then converted to a volume loss using the measured density. Lastly, the specific wear rate ( $mm^3/Nm$ ) was calculated by dividing the volume loss( $mm^3$ ) on both of the applied load(N) and sliding distance (m). Further, the wear coefficient was calculated using Archard equation [19]:

$$\Delta V = K \frac{L \times P}{H} \quad (3)$$

where ( $\Delta V$ ) is the volume loss in  $m^3$ , (L) is the sliding wet wear distance measured by m, (P) is the applied normal load in Newton, (K) is dimensionless wear coefficient, and (H) is the hardness of material by  $N/m^2$ .

## Worn surface

Worn surface of samples after the wear test, was examined with optical microscope and scanning electron microscope (SEM) model (FE-SEM; SEM-JEOL JSM5800-LV), that equipped with a unit of an energy dispersive X-ray spectrometry (EDS). The chemical

composition of tribo-film was identified using EDS and X-ray photoelectron spectroscopy (XPS) analysis model (K-alpha) with Al  $K\alpha$  radiation of 1486.6 eV and chamber pressure less than  $10^{-10}$  Torr.

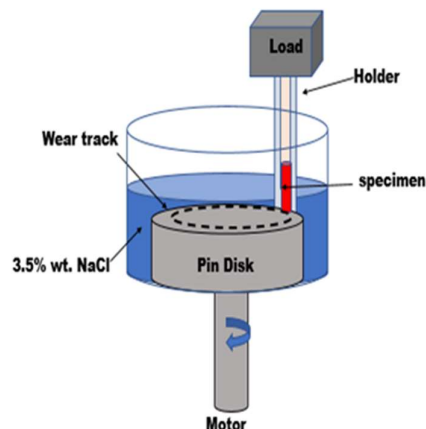


Figure 2 A schematic sketch of pin on the disc wear test set up.

## Results

### Microstructure

The unreinforced AlMg5 alloy and reinforced material structures are shown in Fig.3 (a-d). Clearly Fig.3 (a) shows that the microstructure of the AlMg5 alloy consists of equiaxed grains of aluminum magnesium solid solution ( $\alpha$ -solid solution) and intermetallic phase of  $Al_3Mg_2$  ( $\beta$ -phase) which precipitate mainly along the grain boundaries. The  $Al_3Mg_2$  phases exist in the forms of thin flake ( $\beta$ -  $Al_3Mg_2$ ) and small granule ( $\beta$ -  $Al_3Mg_2$ ) for both the AlMg5 matrix alloy and AlMg5 reinforced with  $ZrO_2$ .

Fig.3(b) shows the uniformly distribution of  $ZrO_2$  particles in the microstructure of the Al-Mg composite. In Fig.3(c), clustered particles are observed in the composite fabricated at casting temperatures of 750  $^{\circ}C$ . It seems that higher fluidity of molten aluminum at a higher casting temperature has affected particle distribution in the composite. Fig.3(d) shows agglomerated particles in the sample reinforced with 15 wt.%  $ZrO_2$  particles, the agglomerated particles are pushed to the last freezing zones. This phenomenon is intensified with increasing particles content in composite.

### XRD analysis

The XRD analysis shows that the base alloy mainly consists of  $\alpha$ -Al solid solution and intermetallic precipitates of  $Al_3Mg_2$ , while the composite contains the same composition as well as  $ZrO_2$  particle as shown in Fig. 4. It is obviously shown that increasing  $ZrO_2$  particles content, the intensity of  $ZrO_2$  peaks increase and the intensity of AlMg5 peaks reduce. The reducing in intensity is attributed to the difference in thermal expansion between AlMg5 matrix and  $ZrO_2$  particles, leading to formation of lattice micro-strain in the matrix. The same behavior is reported by many authors [11,14].

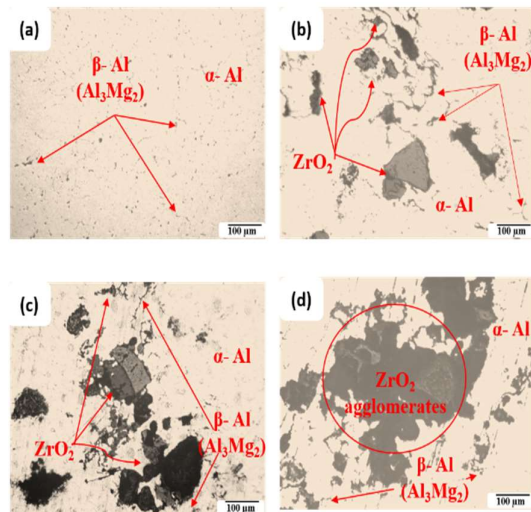


**Figure 3** Microstructure of AlMg5/ZrO<sub>2</sub> composites with different ZrO<sub>2</sub> particles content. (a) 0, (b) 5, (c) 10, and (d) 15 wt.% ZrO<sub>2</sub>.

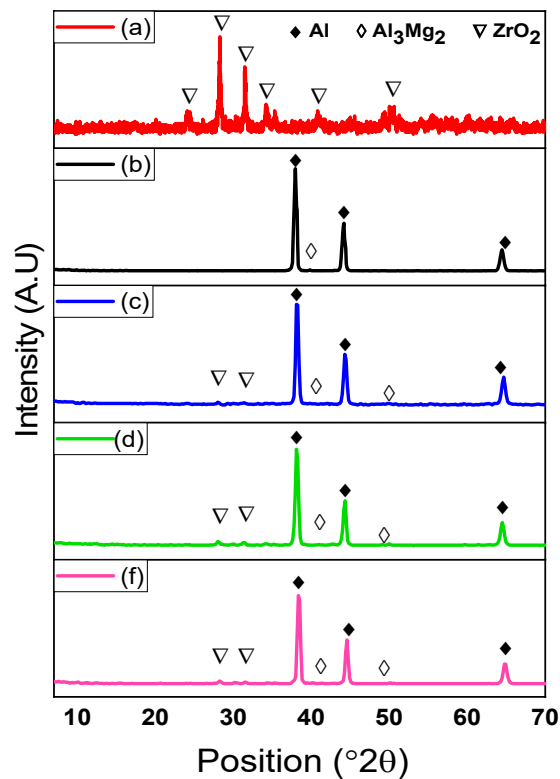


**Figure 4** XRD patterns of ZrO<sub>2</sub> and AlMg5 with different ZrO<sub>2</sub> particles content. (a) ZrO<sub>2</sub> powders, (b) AlMg5, (c) AlMg5/5ZrO<sub>2</sub>, (d) AlMg5/10ZrO<sub>2</sub>, and (e) AlMg5/15ZrO<sub>2</sub>.

### Relative density

It is well known that the properties of MMCs are dependent on the presence of porosity within the obtained composite. Moreover, the density may quantify the metallurgical quality of a material. Therefore, the density of composites is a basic

criterion with which to judge their quality. The effect of ZrO<sub>2</sub> contents on the relative density and porosity level of AlMg5/ZrO<sub>2</sub> composites are shown in Fig. 5. It is clear that increasing ZrO<sub>2</sub> content reduces the relative density of AlMg5/ZrO<sub>2</sub> composites and increases the porosity level. Further Fig.5 indicates that the relative density reduced from 99.28 (AlMg5) to 97.8 % with increasing ZrO<sub>2</sub> particles to 15wt.%. The reduction in the relative density is attributed to the increasing amount of ZrO<sub>2</sub> which agglomerate and increases the porosity level. Formation of porosity sites adjacent to agglomerated particles can affect the mechanical performance of the composite.

The porosity level in composite is slightly greater than that of base matrix, and the same is found to increase with increasing the amount of ZrO<sub>2</sub> as shown in Fig. 5. This behavior is attributed to increment of the viscosity of the melt with addition of ceramic particles which obstruct the reinforcement incorporation and thereby enforce agglomeration and entrapment of more gases [20,21]. Also, the lower latent heat and a high solid fraction in the metal provide quicker melt solidification. This effect in turn reduces the available time for gas escape and thereby increases the porosity level. The porosity is normal, because of the increasing effective viscosity of the suspension and the increase in surface area in contact with air caused by increasing the particle content. This trend is also reported by the early works [22,23] and is attributed to increasing surface gas layers surrounding particles and porosity associated with the particle clusters. Increasing the particle contents increases the probability of clustering ZrO<sub>2</sub> particles. The air trapped in the cluster of particles as well as the hindered liquid metal flow inside them in turn contribute to the formation of porosity.

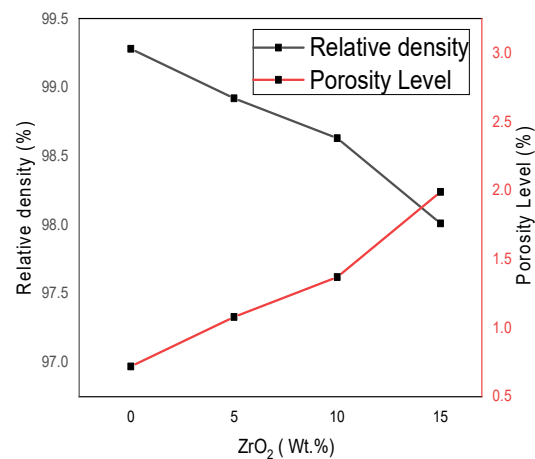


**Figure 5** Effect of ZrO<sub>2</sub> particles content on the relative density and porosity level of AlMg5/ZrO<sub>2</sub> composites.

### Hardness measurements

The average hardness value of composites increases from 59.9 to 82.8 HV with increasing the ZrO<sub>2</sub> contents from 0.0 to 10 wt.%. The average

hardness value of the matrix and composites refers to that the hardness increases with increasing the percentage of  $ZrO_2$  particles up to 10 wt.% and then afterwards rapidly decrease as shown in Fig. 6. The Hardness value for the composite prepared with 10 wt.%  $ZrO_2$  is 38.2% higher than that of the unreinforced aluminum alloy. The increase of hardness can be attributed to the presence of the hard ceramic  $ZrO_2$  particles. Therefore, the strong and rigid  $ZrO_2$  particles severely restrict deformation of the softer AlMg5 matrix in the region adjacent to the boundary. In addition, the reinforcement is attributed to the grain refinement of matrix (Hall mechanism) [24]. Thus, the phase boundaries serve as barriers to dislocation motion in the same way as grain boundaries and the  $ZrO_2$  particles interact with the dislocations of the matrix preventing their movement and consequently, improving the hardness. [25].

Further increase in  $ZrO_2$  contents leads to reduction in hardness values. The hardness of composites reinforced with 15 wt.% is lower than that of the sample reinforced with 5 wt.%  $ZrO_2$  particles. This may be due to the higher porosity content of the composites with increasing  $ZrO_2$  content. It is a result of higher viscosity and increasing tendency to clump the particles together due to high surface tension and poor wetting between the particles and molten alloy. Also, the agglomeration of particle in some regions through the matrix can be considered as the hardness reducing factors [26]. Similar results were obtained by some authors [27-29] who reported that the best hardness value was obtained with about 10% of  $ZrO_2$  and decreases theirs afterwards.

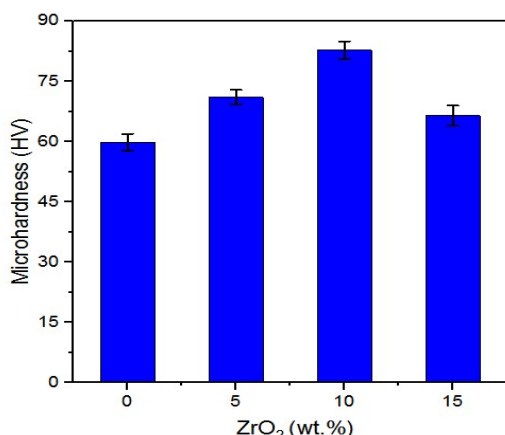


**Figure 6** Effect of  $ZrO_2$  particles content on the hardness of AlMg5/ $ZrO_2$  composites.

## Tribological behaviour

### Effect of sliding speed

The tribological behavior of particulate reinforced MMCs has been generally found to be a function of the applied load as well as the reinforcement content, the shape, and nature of the reinforcing phase. The matrix structure also influences the wear and friction behaviors of MMCs, so that the processing route can enhance the wear resistance of these materials via their effects on the matrix microstructure,

distribution of particles, porosity content, particle matrix bonding and mechanical properties. The variation of the specific wear rates of AlMg5/ $ZrO_2$  composites with different sliding speeds is shown in Fig. 7. It is clear that growing the sliding speed from 0.125 to 0.5  $ms^{-1}$ , the specific wear rate decreases due to decreasing the contact area. At the low sliding speed, the material is removed by the fracture of the reinforcement and matrix due to high frictional force and transferred material layer is also observed. In the intermediate and high speed, the oxide transferred layer has been observed, this layer reduces the direct contact with the hard-counter surface. The adhesive and abrasive wear are the pre-dominant mechanism at low and intermediate speeds, while localizing melting wear at high speed. In addition, increasing the sliding speed, the temperature resulting from friction increases and leads to the formation of a more effective (protective) oxide layer on the surface. Due to the lubricating feature of the emerging oxide layer, the weight loss decreases [2]. Consequently, the lowest specific wear rate obtains at 0.5  $ms^{-1}$  and the highest one obtains at 0.125  $ms^{-1}$ .

Furthermore, Fig. 7 illustrates that the wear rate decreases with increasing  $ZrO_2$  contents from 0.0 to 10 wt.%. The behavior is attributed to  $ZrO_2$  particles act as a load carrier and protect the AlMg5 matrix from damage. Moreover, the results show that incorporating  $ZrO_2$  particles more than 10 wt.%, the wear rate increases but still lower than that of the matrix.

The effect of  $ZrO_2$  contents on the wear coefficient at different sliding speeds is given in Fig. 8. Clearly, the values show that the wear coefficient (K) decreases with the increment of sliding speed. The behavior suggests that the probability of contacting the abrasive material and the investigated alloys decreases with growing sliding speed, leading to producing low sizeable wear particles. Also, Fig. 8 displays that the wear coefficient value decreases with increment the content of  $ZrO_2$  particles up to 10 wt.%. Beyond that, wear coefficient increases due to the agglomeration of  $ZrO_2$  particles and their probability to break off matrix during wear test.

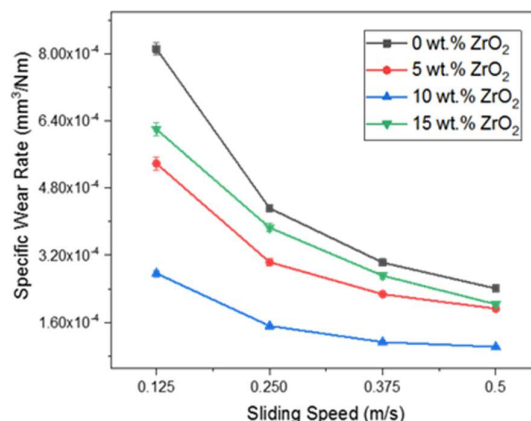


**Figure 7** Effect of sliding speed on the specific wear rate of AlMg5/ $ZrO_2$  composites.

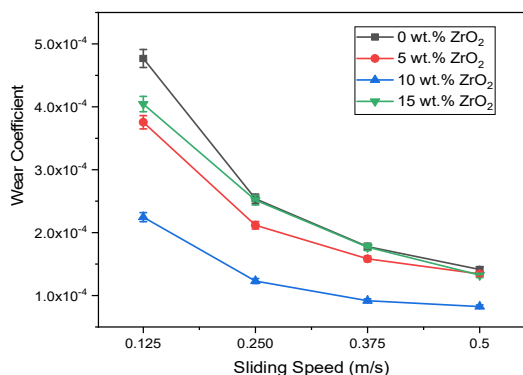


**Figure 8** Effect of sliding speed on the wear coefficient of AlMg5/ZrO<sub>2</sub> composites.

### Effect of load

Fig. 9 shows the effect of load on the specific wear rate of AlMg5/ZrO<sub>2</sub> composites with different percentages of ZrO<sub>2</sub>. There is a linear relationship between wear rate and the applied load. The trend owes to many factors such as: (i) the surface deformation, (ii) removal of load bearing particles (ZrO<sub>2</sub>), (iii) increasing the friction due to the higher contacting couple surface and, faster generation, removal of the tribo-layer and rising the temperature of the surface with increasing the applied load, producing a soft surface. A similar result was obtained by many authors [15,30]. However, the wear resistance of the composites up to 10 wt.% of ZrO<sub>2</sub> increases when compared with the base matrix. This enhancement in wear resistance is attributed to the presence of hard ZrO<sub>2</sub> particles in the AlMg5 matrix which act as protuberances over the surface and protect the soft matrix from severe contact with the abrasive material [11,31]. Furthermore, Fig. 9 shows that beyond the value of 10 wt.% ZrO<sub>2</sub>, the wear resistance decreases due to the agglomeration of ZrO<sub>2</sub> particles. Fig. 10 displays the wear coefficient at different applied loads. It is seen that the wear coefficient decreases with increasing the applied load. This may be due to the formation of transfer film at the contacting surface [32].

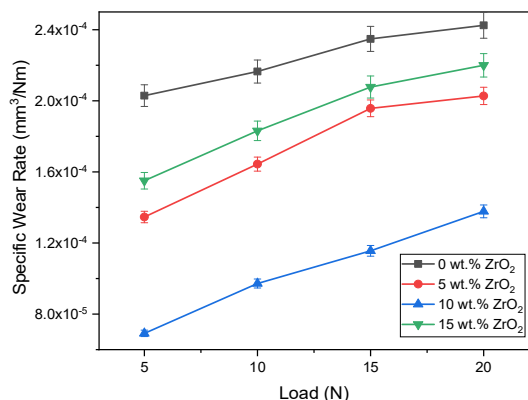


**Figure 9** Effect of applied load on the specific wear rate of AlMg5/ZrO<sub>2</sub> composites.

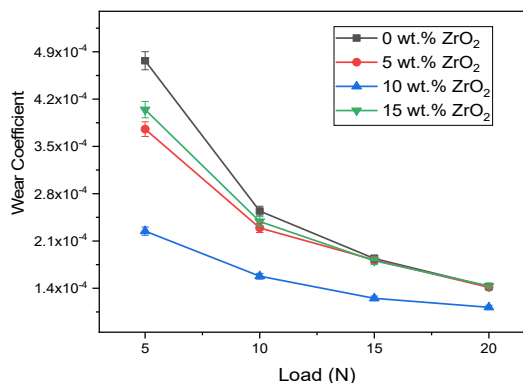


**Figure 10** Effect of applied load on the wear coefficient of AlMg5/ZrO<sub>2</sub> composites.

### Worn surface

Optical micrographs and SEM images were taken for worn surfaces of the investigated samples at an applied load of 15 N, sliding velocity of 0.375 ms<sup>-1</sup> and abrasive particle size of 13 μm, as shown in Figs. 11 and 12. It is obvious that the worn surfaces of all investigated samples are covered with continuous grooves and scratches parallel to the sliding direction. The grooves and scratches resulted from the ploughing action [33]. Also, Fig. 11(a) shows that the grooves are wider and deeper, suggesting an augmented metallic contact and a higher coefficient of friction value. This behavior means that the dominant wear mechanism in AlMg5 sample belongs to the abrasive wear mechanism [21]. Incorporating ZrO<sub>2</sub> as shown in Fig. 11 (b-d) displays that ZrO<sub>2</sub> particles act as protuberance which reduce the contact between the composite and the abrasive material. Figs. 11 and 12 (b-d) show that AlMg5/ZrO<sub>2</sub> composites suffer from abrasive wear, though the presence of ZrO<sub>2</sub> disconnect the continuity of that grooves. Also, the width and depth of grooves decrease with an increment of ZrO<sub>2</sub> to 10 wt.% due to increasing the hardness of these samples. Consequently, beyond that value the width and depth of grooves increase again due to decreasing the hardness. The EDS analysis for AlMg5/10ZrO<sub>2</sub> shows that the tribo-film consists of Al, Mg, Zr, O, Na, and Cl as shown in Fig. 13.

XPS is an effective measurement tool as it indicates what elements are present on the surface and refers to the chemical bonding status on the surface. Fig. 14 represents the XPS outcomes of worn surface. Lorentzian-Gaussian function with Shirley background was utilized to fit the XPS spectra. It is evident that, the peaks centered at about 72.6, 179, and 198.5 eV referred to Al2p, Zr3d5, and Cl2p respectively. Further, the spectrum the peaks located at about 529, 1021.7, 1071, and 1303 eV signifies O1s, Zn2p, Nas, and Mg1s respectively. Therefore, this spectrum is in agreement with the above results.

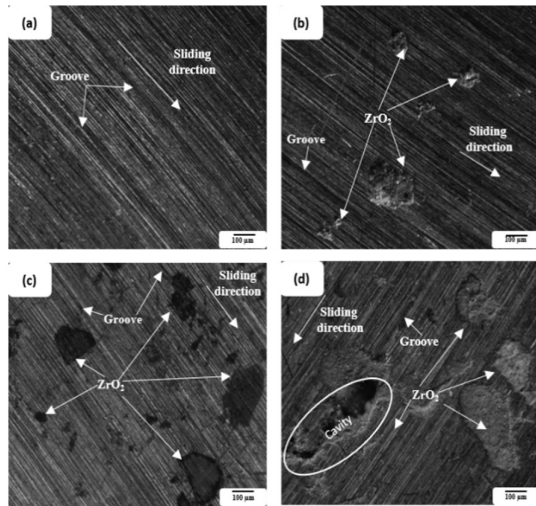


**Figure 11** Optical micrographs of worn surfaces of AlMg5/ZrO<sub>2</sub> composites with different ZrO<sub>2</sub> contents. (a) 0, (b) 5, (c) 10, and (d) 15 wt.% ZrO<sub>2</sub>.

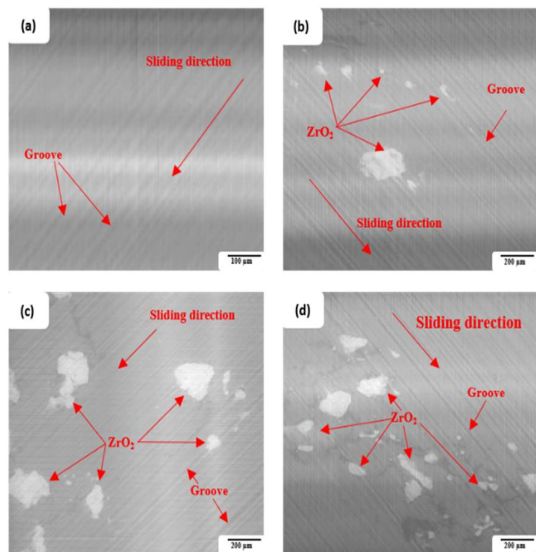


**Figure 12** SEM images of worn surfaces of AlMg5/ZrO<sub>2</sub> composites with different ZrO<sub>2</sub> contents. (a) 0, (b) 5, (c) 10, and (d) 15 wt.% ZrO<sub>2</sub>.

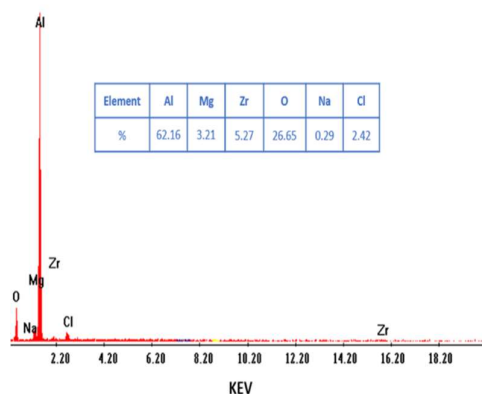


**Figure 13** EDS analysis of AlMg5/10ZrO<sub>2</sub> composite worn surface.

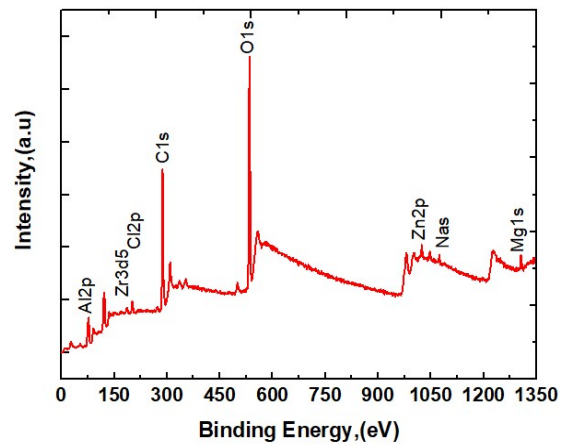


**Figure 14** The representative XPS spectra analysis (survey scan) of AlMg5/10ZrO<sub>2</sub> composite worn surface.

## Conclusions

AlMg5/ZrO<sub>2</sub> composites have been successfully manufactured via stir casting technique. The microstructure and tribological behavior have been investigated. The obtained conclusions can be summarized as follows:

1. The relative density decreased by increasing the ZrO<sub>2</sub> particles content while the porosity level increased.
2. Hardness and wear resistance of AlMg5 alloy significantly augmented with ZrO<sub>2</sub> addition up to 10 wt.%, beyond this value the hardness and wear resistance diminished but still higher than the base matrix.
3. The specific wear rate of AlMg5 and its composites decreased linearly with increasing sliding speed. However, the sample contains 10 % gives the lowest specific wear rate.
4. The specific wear rate of all investigated samples incremented with increasing the applied load.
5. The dominant wear mechanism in AlMg5 alloy and AlMg5/ZrO<sub>2</sub> composites was abrasive wear.

## Funding sources

This research received no external funding.

## Conflicts of interest

There are no conflicts to declare.

## References

- [1] J. Hashim, L. Looney, and M. S. J. Hashmi, "Particle Distribution in Cast Metal Matrix Composites-Part I," *J. Mater. Process. Technol.*, vol. 123, no. 2, pp. 251–257, 2002.
- [2] İ. Şimşek, D. Şimşek, and D. Özyürek, "The Effect of Different Sliding Speeds on Wear Behavior of ZrO<sub>2</sub> Reinforcement Aluminium Matrix Composite Materials," *Int. Adv. Res. Eng. J.*, vol. 4, no. 1, pp. 1–7, 2020.
- [3] G. Moona, R. S. Walia, V. Rastogi, and R. Sharma, "Aluminium Metal Matrix Composites: A Retrospective

- Investigation," *Indian J. Pure Appl. Phys.*, vol. 56, no. 2, pp. 164–175, 2018.
- [4] A. K. Sharma, R. Bhandari, A. Aherwar, R. Rimašauskienė, and C. Pinca-Bretotean, "A Study of Advancement in Application Opportunities of Aluminum Metal Matrix Composites," *Mater. Today Proc.*, vol. 26, pp. 2419–2424, 2020.
- [5] L. Ceschini et al., *Aluminum and Magnesium Metal Matrix Nanocomposites*. 2017.
- [6] M. Metwally, M. Sadawy, and I. EL-Batanony, "Effect of SiC (p) Content on The Corrosion Behavior of Nano SiC (p)/Cu Composites," *Egypt. J. Eng. Sci. Technol.*, vol. 26, no. EIJEST, Vol. 26, 2018, pp. 22–28, 2018.
- [7] A. Kandil, "Fabrication and Characterization of Metal Matrix Composites Reinforced with Al<sub>2</sub>O<sub>3</sub>-fibers," *Metall.*, vol. 59, no. 3, pp. 119–124, 2005.
- [8] B. Dikici, F. Bedir, and M. Gavali, "The Effect of High Tic Particle Content on The Tensile Cracking and Corrosion Behavior of Al–5Cu Matrix Composites," *J. Compos. Mater.*, vol. 54, no. 13, pp. 1681–1690, 2020, doi: 10.1177/0021998319884098.
- [9] A. Mourad, E. S. Mousa, and A. Kandil, "Fabrication of AA6082/WC Nanocomposite by Friction Stir Processing and Optimization Using Taguchi Approach," *J. Al-Azhar Univ. Eng. Sect.*, vol. 15, no. 57, pp. 1030–1039, 2020.
- [10] S. Sakthivelu, P. P. Sethusundaram, M. Meignanamoorthy, and M. Ravichandran, "Synthesis of Metal Matrix Composites Through Stir Casting Process - A Review," *Mech. Mech. Eng.*, vol. 22, no. 1, pp. 357–369, 2018.
- [11] M. S. Abd-Elwahed, A. F. Ibrahim, and M. M. Reda, "Effects of ZrO<sub>2</sub> Nanoparticle Content on Microstructure and Wear Behavior of Titanium Matrix Composite," *J. Mater. Res. Technol.*, vol. 9, no. 4, pp. 8528–8534, 2020.
- [12] M. Ramachandra, A. Abhishek, P. Siddeshwar, and V. Bharathi, "Hardness and Wear Resistance of ZrO<sub>2</sub> Nano Particle Reinforced Al Nanocomposites Produced by Powder Metallurgy," *Procedia Mater. Sci.*, vol. 10, no. Cnt 2014, pp. 212–219, 2015, doi: 10.1016/j.mspro.2015.06.043.
- [13] A. Kandil, "Fabrication and Characterization of Magnesium Alloy (AZ91) Metal Matrix Composites Reinforced with SiC-Particles," *Metall-Clausthal*, vol. 66, no. 1, p. 33, 2012.
- [14] V. Khalili, A. Heidarzadeh, S. Moslemi, and L. Fathyunes, "Production of Al6061 Matrix Composites with ZrO<sub>2</sub> Ceramic Reinforcement Using a Low-Cost Stir Casting Technique: Microstructure, mechanical properties, and electrochemical behavior," *J. Mater. Res. Technol.*, vol. 9, no. 6, pp. 15072–15086, 2020, doi: 10.1016/j.jmrt.2020.10.095.
- [15] G. B. V. Kumar, R. Pramod, C. G. Sekhar, G. P. Kumar, and T. Bhanumurthy, "Investigation of Physical, Mechanical and Tribological Properties of Al6061–ZrO<sub>2</sub> Nano-Composites," *Heliyon*, vol. 5, no. 11, p. e02858, 2019.
- [16] M. A. Baghchesara, H. Abdizadeh, and H. R. Baharvandi, "Fractography of Stir Casted Al-ZrO<sub>2</sub> Composites," *Iran. J. Sci. Technol. Trans. B Eng.*, vol. 33, no. 5, pp. 453–462, 2009.
- [17] Hashmi, J., "The Production of Metal Matrix Composites Using the Stir Casting By," *J. Mater. Process. Technol.*, vol. 92–93, pp. 1–7, 1999.
- [18] A. S. Rathaur, J. K. Katiyar, and V. K. Patel, "Experimental Analysis of Mechanical and Structural Properties of Hybrid Aluminium (7075) Matrix Composite Using Stir Casting Method," in *IOP Conference Series: Materials Science and Engineering*, 2019, vol. 653, no. 1, p. 12033.
- [19] M. A. Metwally, M. M. Sadawy, M. Ghanem, and I. G. EL-Batanony, "The Role of Nano-SiC on Microstructure and Tribological Properties of SiC/Cu Nano-Composite," *J. Eng. Res. Reports*, pp. 35–44, 2020.
- [20] S. Sardar, S. K. Karmakar, and D. Das, "Microstructure and Tribological Performance of Alumina-Aluminum Matrix Composites Manufactured by Enhanced Stir Casting Method," *J. Tribol.*, vol. 141, no. 4, 2019, doi: 10.1115/1.4042198.
- [21] J. Suthar and K. M. Patel, "Processing Issues, Machining, and Applications of Aluminum Metal Matrix Composites," vol. 6914, no. November 2017, doi: 10.1080/10426914.2017.1401713.
- [22] A. M. Samuel, A. Gotmare, and F. H. Samuel, "Effect of Solidification Rate and Metal Feedability on Porosity and SiC/Al<sub>2</sub>O<sub>3</sub> Particle Distribution in an Al-Si-Mg (359) Alloy," *Compos. Sci. Technol.*, vol. 53, no. 3, pp. 301–315, 1995.
- [23] M. Gupta, M. O. Lai, M. S. Boon, and N. S. Heng, "Regarding the SiC Particulates Size Associated Microstructural Characteristics on the Aging Behavior of Al–4.5 Cu Metallic Matrix," *Mater. Res. Bull.*, vol. 33, no. 2, pp. 199–209, 1998.
- [24] J. Corrochano, M. Lieblich, and J. Ibáñez, "On the Role of Matrix Grain Size and Particulate Reinforcement on the Hardness of Powder Metallurgy Al–Mg–Si/MoSi<sub>2</sub> Composites," *Compos. Sci. Technol.*, vol. 69, no. 11–12, pp. 1818–1824, 2009.
- [25] B. P. Beyrami, H. Abdizadeh, H. R. Baharvandi, and M. A. M. Bonab, "The Effect of Composition and Stir-Casting Parameters on the Mechanical Properties of Al / ZrO<sub>2</sub>p."
- [26] T. Satish Kumar, S. Shalini, and K. Krishna Kumar, "Synthesis and Characterization of Al-Zn-Mg Alloy / Zircon Sand Reinforced Composites," *Arch. Metall. Mater.*, vol. 63, no. 2, pp. 689–695, 2018, doi: 10.24425/122395.
- [27] S. Udayashankar and V. S. Ramamurthy, "Development and Characterization of Al6061-Zirconium Dioxide Reinforced Particulate Composites," *Int. J. Eng. Technol.*, vol. 7, no. 3, pp. 128–132, 2018.
- [28] P. Chinna, S. Rao, T. Prasad, and M. Harish, "Evaluation of Mechanical Properties of Al 7075 – ZrO<sub>2</sub> Metal Matrix Composite by Using Stir Casting Technique," *Int. J. Sci. Res. Eng. Technol.*, vol. 6, no. 4, pp. 2278–882, 2017.
- [29] H. Abdizadeh and M. A. Baghchesara, "Investigation on Mechanical Properties and Fracture Behavior of A356 Aluminum Alloy Based ZrO<sub>2</sub> Particle Reinforced Metal-Matrix Composites," *Ceram. Int.*, vol. 39, no. 2, pp. 2045–2050, 2013, doi: 10.1016/j.ceramint.2012.08.057.
- [30] M. Metwally, H. A. Fattah, M. Ghanem, and I. Batanony, "Effect of SiC Content on Dry Sliding Wear Behavior of Nanosized SiC (P)/Cu Composites," *J. Al-Azhar Univ. Eng. Sect.*, vol. 13, no. 49, pp. 1260–1267, 2018.

- 
- [31] M. Rahimian, N. Parvin, and N. Ehsani, "The Effect of Production Parameters on Microstructure and Wear Resistance of Powder Metallurgy Al-Al<sub>2</sub>O<sub>3</sub> Composite," *Mater. Des.*, vol. 32, no. 2, pp. 1031–1038, 2011.
- [32] M. Singla, L. Singh, and V. Chawla, "Study of Wear Properties of Al-SiC Composites," *J. Miner. Mater. Charact. Eng.*, vol. 8, no. 10, pp. 813–819, 2009.
- [33] M. Sadawy, "The Influence of Heat Treatment on Tribological Properties of Cu-Al-Fe-Ni Shape Memory Alloy," *Egypt. J. Eng. Sci. Technol.*, vol. 29, no. EIJEST, Vol. 29, 2020, pp. 45–50, 2020.